

# Wavelength Dependence of the Ocular Straylight

Harilaos S. Ginis,<sup>1</sup> Guillermo M. Perez,<sup>2</sup> Juan M. Bueno,<sup>1</sup> Alexandros Pennos,<sup>1</sup> and Pablo Artal<sup>1</sup>

<sup>1</sup>Laboratorio de Optica, Universidad de Murcia, Murcia, Spain

<sup>2</sup>Voptica SL, Murcia, Spain

Correspondence: Harilaos S. Ginis, Laboratorio de Optica (LO-UM), Instituto Universitario de investigación en Óptica y Nanofísica (IUioyN), Universidad de Murcia, Campus de Espinardo (Edificio 34), 30100 Murcia, Spain; ginis@um.es.

Submitted: January 21, 2013

Accepted: April 4, 2013

Citation: Ginis HS, Perez GM, Bueno JM, Pennos A, Artal P. Wavelength dependence of the ocular straylight. *Invest Ophthalmol Vis Sci*. 2013;54:3702-3708. DOI:10.1167/iov.13-11697

**PURPOSE.** Ocular straylight is the combined effect of light scattering in the optical media and the diffuse reflectance from the various fundus layers. The aim of this work was to employ an optical technique to measure straylight at different wavelengths and to identify the optimal conditions for visually relevant optical measurements of straylight.

**METHODS.** The instrument, based on the double-pass (DP) principle, used a series of uniform disks that were projected onto the retina, allowing the recording of the wide-angle point spread function (PSF) from its peak and up to  $7.3^\circ$  of visual angle. A liquid crystal wavelength tunable filter was used to select six different wavelengths ranging from 500 to 650 nm. The measurements were performed in nine healthy Caucasian subjects. The straylight parameter was analyzed for small ( $0.5^\circ$ ) and large ( $6^\circ$ ) angles.

**RESULTS.** For small angles, the wavelength dependence of straylight matches the transmittance spectrum of hemoglobin, which suggests that diffuse light from the fundus contributes significantly to the total straylight for wavelengths longer than 600 nm. Eyes with lighter pigmentation exhibited higher straylight at all wavelengths. For larger angles, straylight was less dependent on wavelength and eye pigmentation.

**CONCLUSIONS.** Small-angle straylight in the eye is affected by the wavelength-dependent properties of the fundus. At those small angles, measurements using wavelengths near the peak of the spectral sensitivity of the eye might be better correlated with the visual aspects of straylight. However, the impact of fundus reflectance on the values of the straylight parameter at larger angles did not depend on the measuring wavelength.

**Keywords:** straylight, wavelength, physiological optics

Ocular straylight affects retinal image quality by casting a veiling glare over the retinal image, especially in the presence of one or more bright sources in the visual field.<sup>1,2</sup> Straylight is the combined effect of light scattering in the optical media of the eye and diffusion of light at the various layers of the fundus. In particular, scattering typically occurs as light interacts with random inhomogeneities located in the optical media of the eye. Moreover, light diffused at the fundus as well as light propagating through the ocular wall may contribute to increase the overall scattered light on the retinal plane.<sup>2-5</sup>

There is experimental evidence that light scattering in ex vivo donor corneas has wavelength dependence similar to Rayleigh scattering,<sup>6</sup> increasing at shorter wavelengths. Measurements with donor crystalline lenses revealed a similar wavelength dependence, although weaker than in the cornea.<sup>7,8</sup>

Despite these ex vivo findings, functional measurements of straylight using psychophysical techniques have not shown a significant wavelength dependence.<sup>9,10</sup> Using a refined psychophysical test,<sup>11</sup> Coppens and coauthors found small but systematic differences across wavelengths within the visible spectrum.<sup>12</sup> However, the study took into account only scatter angles greater than  $3.5^\circ$ .

Straylight in the human eye is usually described with psychophysically derived empirical formulas. IJspeert and coauthors,<sup>13</sup> as well as Vos and van den Berg,<sup>14</sup> have provided a review of these empirical formulas supplemented with

semitheoretical considerations to provide equations that take into account the eye's age and pigmentation. The essence of these formulas is the inverse angle square law connecting the eye's point spread function (PSF) and glare angle, also known as the Stiles-Holladay glare function.<sup>1,15</sup> Often, based on the Stiles-Holladay law, the value of the PSF at a given angle is multiplied by the square of that angle to derive a quantity (called "straylight parameter") as an indicator of the straylight intensity (or equivalent luminance when derived psychophysically).<sup>16</sup>

The purpose of this study was to use a new optical technique<sup>17</sup> based on the double-pass method<sup>18</sup> to study the wavelength dependence of straylight at angles ranging from  $0^\circ$  to  $7.3^\circ$  in a group of healthy subjects. The method uses extended sources, as well as appropriate image-processing methods, and optimizes the experimental conditions for visually relevant optical measurements of straylight in the human eye. The use of extended sources (uniform disks) projected sequentially enhances the sensitivity of the double-pass technique and extends the measurement to angles at which the PSF is seven orders of magnitude lower than the peak.<sup>17</sup>

## METHODS

### Experimental Setup

The experimental setup was based on a previously described instrument<sup>17</sup> that is depicted schematically in Figure 1. Briefly,

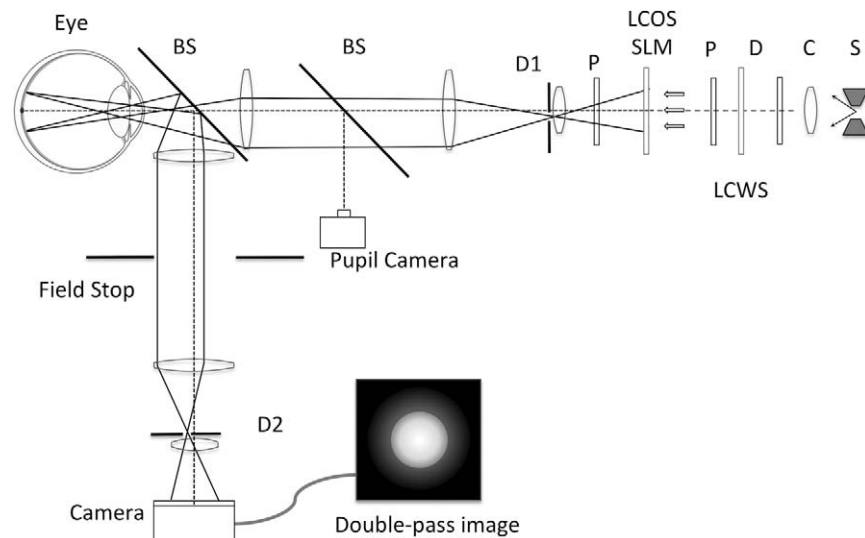


**FIGURE 1.** Schematic of the experimental system. S, xenon lamp; C, condenser lens; D, diffusers; P, linear polarizers; D1 and D2, diaphragms; LCWS, liquid crystal selectable bandwidth tunable optical filter; LC-SLM, liquid crystal modulator; BS, beam splitter.

a liquid crystal spatial light modulator (LC 2002; Holoeye, Berlin-Adlershof, Germany), back-illuminated by a xenon lamp (S) through appropriate condenser lens (C) and light-shaping diffusers (D), produces uniformly illuminated disks. A selectable bandwidth tunable optical filter (LCWS; Meadowlark Optics, Inc., Frederick, CO) was used to select different wavelength bands centered at 500, 550, 570, 600, 630, and 650 nm. The full-width half-maximum of the bands selected was approximately 35 nm. Through appropriate optics the different disks were projected onto the retina. A similar optical design was used in the recording pathway to image the retinal disk onto an electron multiplying charge-coupled device camera (EMCCD Luca; Andor, Belfast, UK).

Two diaphragms, D1 and D2, both conjugated to the pupil plane, are displaced transversely to each other so that the upper part of the pupil is used for projection (first pass, illumination pathway) and the lower part is used for recording (second pass, recording pathway). These two diaphragms have diameters equal to 1.8 mm, and their centers are separated by 4 mm at the pupil plane. As the two subapertures are spatially separated at the pupil plane, back-scattered light from both the cornea and the lens is removed, and it does not contribute to the recorded images of the disks on the retina. Besides separating the illumination and imaging arm, the small diaphragms practically eliminate the role of aberrations and small refractive errors to the peripheral part of the PSF.

### Measurement Procedure

For each measurement, a series of 50 uniform disks was projected and the corresponding fundus images were recorded. Disk projection and image recording were synchronized via scripts developed for this purpose in MATLAB (The Mathworks, Inc., Natick, MA). The disk radii ranged from  $0.18^\circ$  to  $7.3^\circ$ .

For each recorded double-pass image, the intensity at the center of each disk was computed by averaging the central  $5 \times 5$  pixel area. The nonlinear camera's (EMCCD Luca; Andor) response at the particular settings used here was measured in a previous calibration operation. This response was taken into account by applying the respective nonlinear intensity transformation to the recorded images.

Nine Caucasian subjects (age range, 25–51 years; mean, 34 years) with no known ocular or systematic pathology were enrolled in the measurements. Two drops of tropicamide 1% (15 minutes apart) were instilled to each tested eye for pupil dilation. The pupil was aligned by means of a pupil camera (Hercules Classic Webcam; Guillemot Corporation, La Gacilly Cedex, France). The head was stabilized by means of a bite bar. The subjects fixated on a target at a direction of approximately  $7^\circ$  nasally, and that was further adjusted to avoid large retinal blood vessels at (or near) the center of the projected disks during initial trial images. For each wavelength, the sequence of 50 disks was recorded in a randomized order. The subjects were given time to blink between consecutive images. The irradiance at the corneal plane was below  $25 \mu\text{W}/\text{cm}^2$  for all wavelengths.

For some aspects of the analysis that follows, the eyes were divided into two groups with respect to their anterior iris pigmentation: dark and light. However, this classification was made solely by visual observation. No attempt was made to assess the density of melanin in these eyes or to derive quantitative dependence of straylight on pigmentation.

The experiment followed the tenets of the Declaration of Helsinki. Informed consent was obtained from the subjects after they were fully informed about the nature of the measurements.

### Data Analysis

The key observation behind the measurement method and data analysis is that the normalized intensity (with respect to full-field illumination) at the center of a disk with radius  $\theta$  is equal to the radial integral of the PSF of the system between 0 and  $\theta$ .<sup>17</sup> Then, the PSF can be calculated from the derivative of the central intensity of the disks for each series with respect to  $\theta$  by using the following equation<sup>17</sup>:

$$dp\text{PSF}(\theta) = \frac{1}{2\pi\theta} \frac{dI_c(\theta)}{d\theta} \quad (1)$$

where  $I_c(\theta)$  is the central intensity of the recorded disk and  $\theta$  is the disk diameter. To avoid noise associated with numerical differentiation, an appropriate function was fitted to the experimental data (see below), and the derivative was evaluated analytically. The PSF was assumed to be rotationally

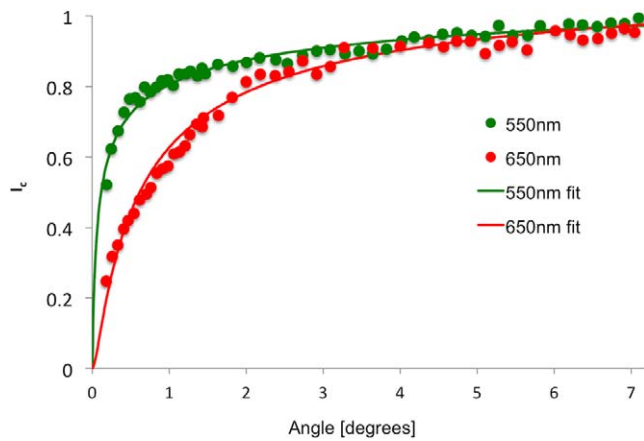


**FIGURE 2.** Normalized central intensity of the disks projected onto the retina and recorded in double pass for one subject (GP) at 550 and 650 nm. The *solid lines* correspond to the fitted functions that were used to compute the underlying PSF.

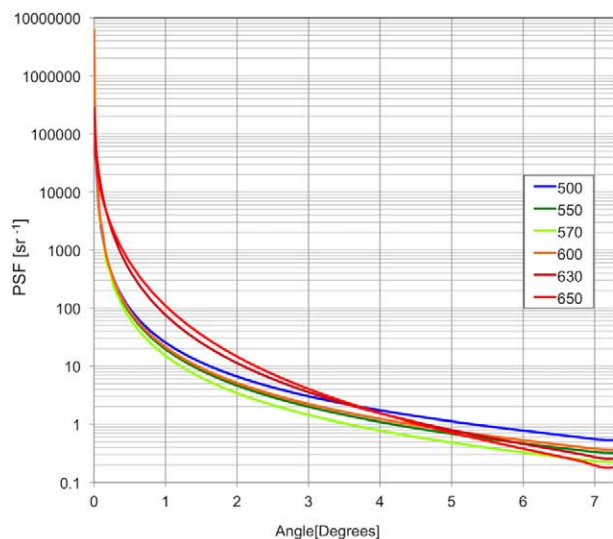
symmetric, and the following formula was used to approximate its shape:

$$dpPSF = \frac{a}{(\theta + \theta_o)^n} \quad (2)$$

where  $\theta_o$  and  $n$  are arbitrary constants and  $\alpha$  is a normalization coefficient (which depends on  $\theta_o$  and  $n$ ) so that the radial integral of the PSF is equal to unity. Similar generalizations of the Stiles-Holladay formula have been previously employed to approximate the PSE<sup>19,20</sup>. This function has the flexibility to approximate different values of the PSF at its most peripheral parts while  $\theta_o$  can be adjusted to match different widths of the central part of the PSF.

The radial integral of this function was used to fit the experimental data:

$$I_c = \int_0^\theta 2\pi\varphi \frac{\alpha}{(\varphi + \theta_o)^n} d\varphi \quad (3)$$



As experimental data on  $I_c$  are recorded in arbitrary units, they are normalized in the fitting process so their range is between 0 and 1. Figure 2 shows normalized data and fitted functions.

The double-pass PSF was reconstructed based on the estimated values of  $\theta_o$  and  $n$ . This creates by definition (Equation 2) a double-pass PSF that is radially normalized to unity.

The (single-pass) PSF was calculated numerically by considering that the double-pass PSF (*dpPSF*) is the autocorrelation of the PSE:

$$PSF = \mathcal{F}^{-1} \left[ \sqrt{|\mathcal{F}(dpPSF)|} \right] \quad (4)$$

where  $\mathcal{F}$  and  $\mathcal{F}^{-1}$  denote the two-dimensional discrete Fourier transform and its inverse, respectively. For each reconstructed PSF, the “straylight parameter”  $PSF(\theta) \cdot \theta^2$  was calculated for  $0.5^\circ$  and  $6^\circ$  to quantify narrow- and wider-angle scattering, respectively.

## RESULTS

Figure 3 shows typical wide-angle PSFs reconstructed from two eyes at six different wavelengths. It is interesting to observe that the PSFs for each subject are very similar for wavelengths between 500 and 600 nm. However, for 630 and 650 nm, these PSFs significantly increased (approximately by a factor of 5) especially for angles up to  $4^\circ$ .

This finding is more clearly illustrated in Figure 4 where the average (across subjects) straylight parameter ( $\theta^2 \cdot PSF(\theta)$ ) is plotted for different wavelengths. Small-angle scattering has a strong wavelength dependence characterized by an abrupt increase for wavelengths longer than 600 nm. The dependence was similar in eyes with dark and light pigmentation (upper panels). At wider angles ( $6^\circ$ ), the straylight parameter did not exhibit this marked increase at longer wavelengths. However, for eyes with light pigmentation, a minimum in the straylight parameter between 550 and 600 nm was observed. This also occurred when the straylight parameter was averaged for all subjects involved in the study (see Fig. 5).

Figure 6 shows the relationship between straylight parameter at  $6^\circ$  and straylight parameter at  $0.5^\circ$  for short and long wavelengths (each data point corresponds to one subject).

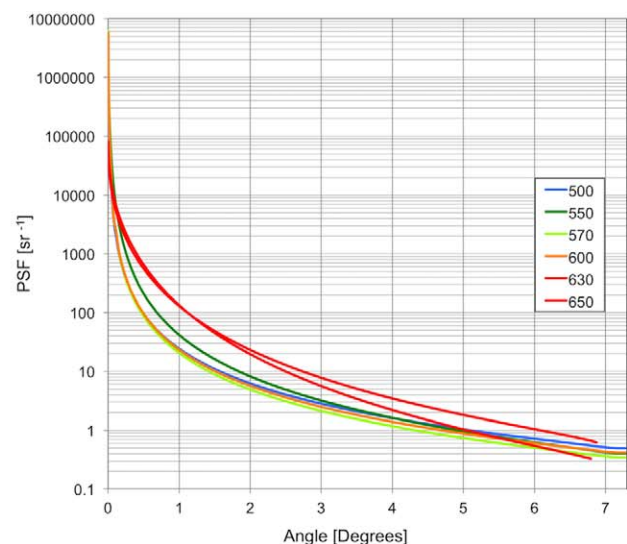


**FIGURE 3.** Reconstructed wide-angle PSFs for two eyes and different wavelengths. *Left:* HG (dark pigmentation, age 43); *right:* PA (light pigmentation, age 51).

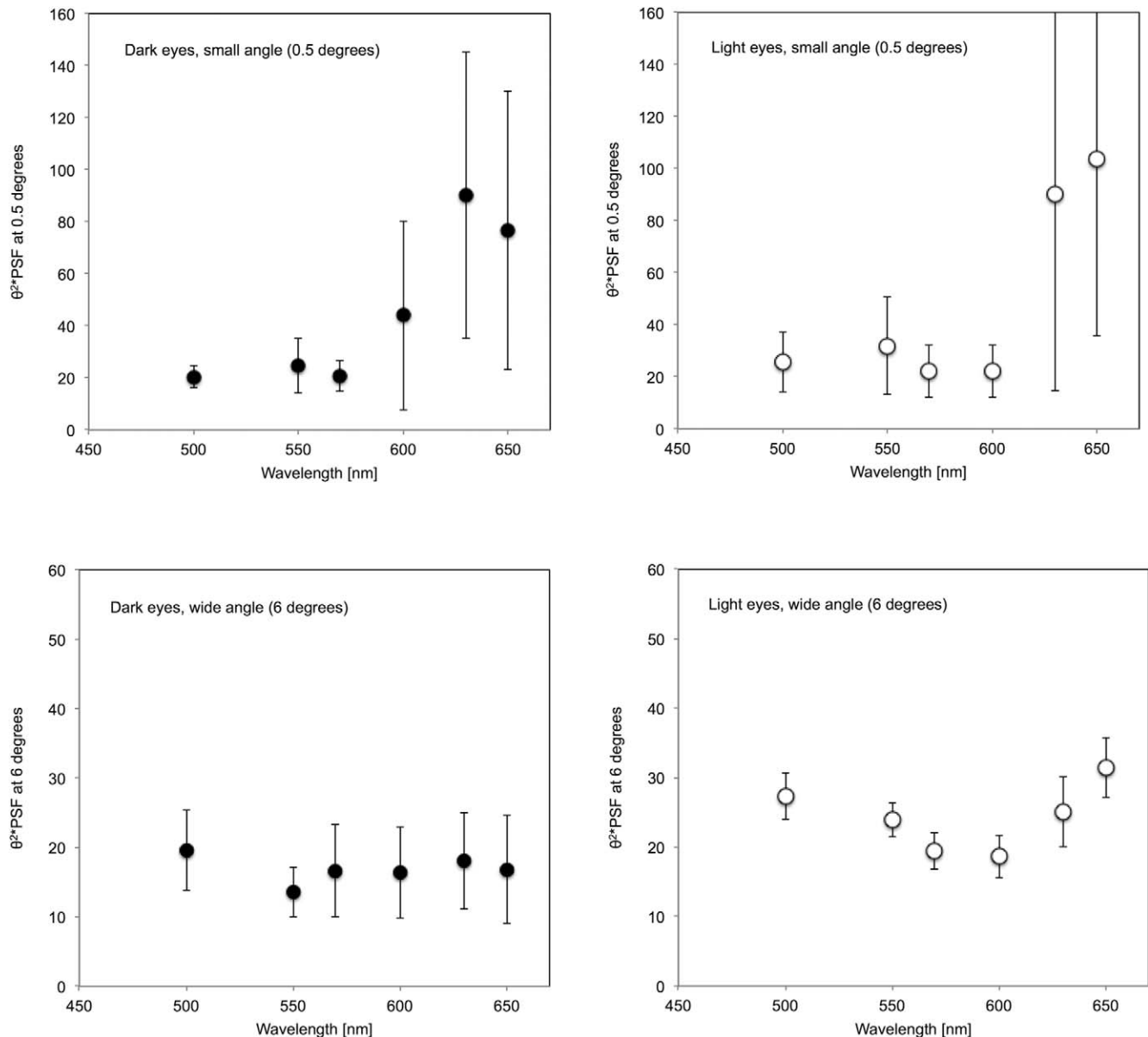


FIGURE 4. Straylight parameter as a function of wavelength calculated for small angles (*top*) and wide angles (*bottom*) and for two groups of eyes, those with dark pigmentation (*left*) and those with lighter pigmentation (*right*).

Although no statistically significant correlation was observed, the variability for longer wavelengths was higher. This indicates that the PSF deviates from the Stiles-Holladay approximation for this angle range including the very small angles ( $0.5^\circ$ ), especially at longer wavelengths.

## DISCUSSION

Our measurements of straylight using an all-optical method allowed the reconstruction of the PSF in the human eye in a wide range of angles (up to  $7.3^\circ$ ) for six different wavelengths (between 500 and 650 nm). The use of small diaphragms in the illumination and imaging pathways ensured that any chromatic focal shift would have negligible effect in the zones of the PSF that were analyzed. The PSF in relation to the ocular scattering as recorded by using the methodology explained above is a result of the combined effects of light scattering in the optics and light diffused at the fundus. Additionally, light after

multiple reflections at the ocular wall may cause a relatively uniform background.

Although in real glare conditions an additional component associated with the translucency of the pupil and the sclera may be involved,<sup>4,12</sup> this was not the case in our measurements, as all the illumination light was delivered through a small subaperture of the pupil. Our measurement technique cannot segregate the relative contribution of different mechanisms in total straylight. The discussion below, comparing our findings with those of earlier studies, is mostly of qualitative nature.

Figure 7 shows the average straylight parameter calculated at  $0.5^\circ$  as a function of wavelength plotted (in arbitrary scale) with oxyhemoglobin density,<sup>21</sup> fundus reflectance as measured by Delori and Pflibsen,<sup>22</sup> and the standard deviation (referring to its spatial extent) of the PSF associated with a model of diffusion at the fundus as suggested by Hodgkinson et al.<sup>23</sup> Although the total optical properties of the fundus are

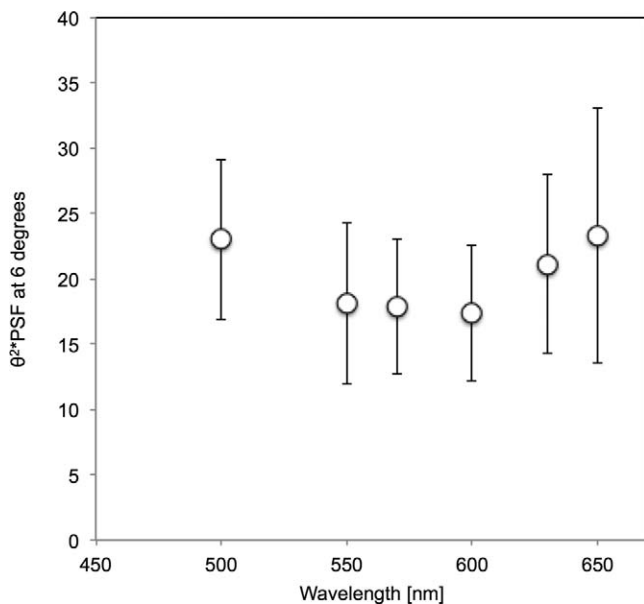
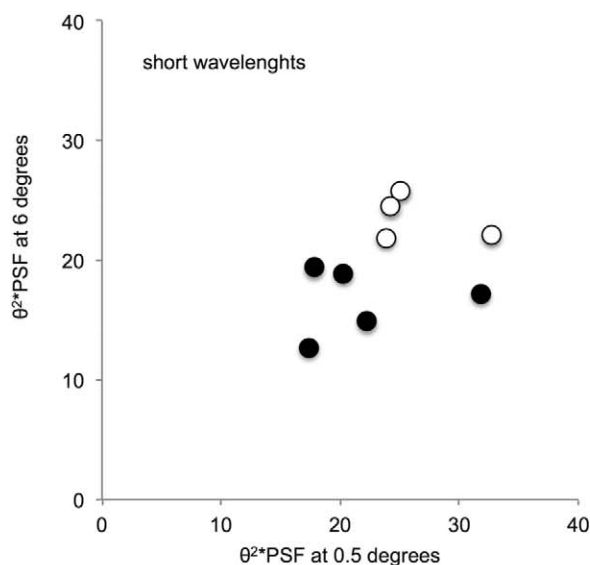


FIGURE 5. Straylight parameter at 6° as a function of wavelength averaged for all subjects.

influenced by other pigments (i.e., melanin and the visual pigments), it seems that our findings for the small-angle PSF are consistent with the hypothesis that hemoglobin is acting as a major absorber in the fundus. Figure 8 shows the ratio of the PSF at “red” wavelengths (630 and 650 nm) to the PSF at “green” wavelengths (550 and 570 nm) averaged for all eyes and plotted as a function of angle. This analysis indicates that the spatial extent of diffuse light is practically limited to approximately 4°. We hypothesize that the variability of this ratio is associated with the variability of melanin density in the fundus.

$$PSF_{red}/PSF_{green} = \frac{PSF_{630} + PSF_{650}}{PSF_{550} + PSF_{570}} \quad (5)$$



For wider angles, the PSF is mainly produced by light scattered at the eye’s optics, with a possible contribution from background light multiply reflected in the interior of the ocular wall—especially in eyes with lighter pigmentation. The observation of practically limited diffusion at the fundus is in line with the theoretical analysis of the diffusion equations for reflectance from a semi-infinite turbid medium as described by Kienle and Patterson.<sup>24</sup> These steady-state solutions involve exponential terms<sup>24</sup> that have naturally a steeper decay than the power law expected for the peripheral part of the PSF. The formalism of Kienle and Patterson<sup>24</sup> may be useful for the development of a model of straylight in the human eye.

Moreover, it is interesting to observe in Figure 5 (straylight parameter calculated at 6° and averaged across all subjects) that the absolute minimum of straylight occurs near the peak of the photopic spectral sensitivity of the eye followed by an increase at wavelengths longer than 600 nm. This finding is in accordance with the psychophysical data of Coppens et al.<sup>12</sup> indicating that diffuse light in the fundus contributes to the straylight values measured psychophysically. Additionally this finding is also supported by earlier findings of Berendschot et al.<sup>25</sup> where the wavelength dependence of the Stiles-Crawford effect explained on the basis of perception of backscattered light from the choroid.

However, the finding that small-angle (0.5°) straylight can be five times higher in the red part of the visible spectrum compared to that in the green leads to the paradoxical prediction that glare from white sources should appear as having a red hue. The role of straylight in chromatic induction<sup>20</sup> and the associated lateral effects in vision may have to be further investigated in view of this observation.

Straylight in the human eye occurs as scattering both at its optical media and at the fundus as a result of diffuse reflectance. Given its strong wavelength dependence, diffusion at the fundus seems to be the primary contribution to straylight for young and healthy eyes where small angles (0.5°) of straylight and wavelengths longer than 600 nm are concerned.

Optical measurements of straylight at shorter wavelengths, and in particular near the peak of the photopic spectral sensitivity of the eye, may be more suitable for the

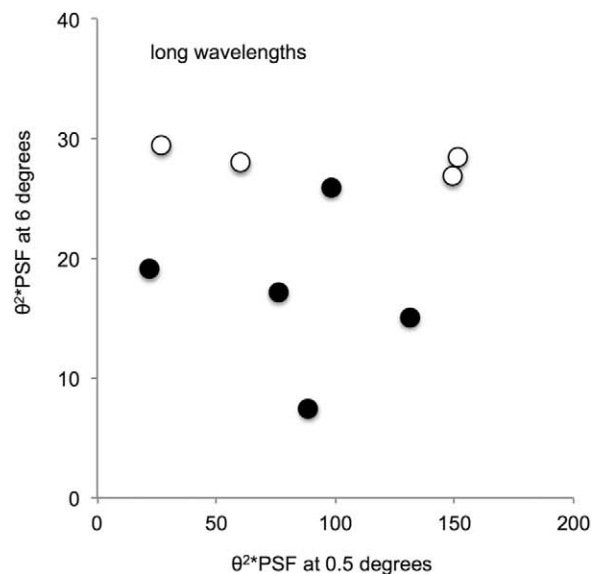


FIGURE 6. Correlation between the straylight parameter at 6° and 0.5° for (left) short wavelengths (average of 500, 550, and 570 nm) and (right) long wavelengths (average of 500, 550, and 570 nm) and (right) “long” wavelengths (average of 630 and 650 nm). Black and white symbols correspond to eyes with dark and light pigmentation.

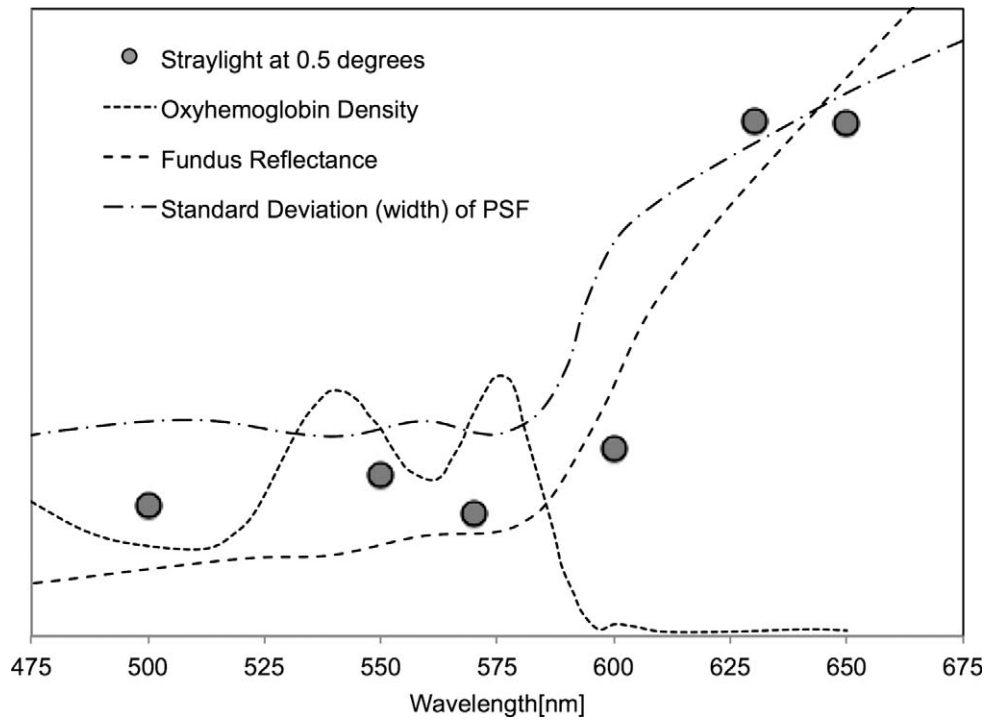


FIGURE 7. Straylight parameter at 0.5° (average of all subjects) and other spectral properties of the fundus. Oxyhemoglobin density is from Berendschot al.,<sup>21</sup> fundus reflectance from Delori and Pflibsen,<sup>22</sup> and the standard deviation (width) of the PSF from Hodgkinson et al.<sup>23</sup>

characterization of image quality and the study of glare phenomena in the eye.

Instruments based on the near-angle double-pass technique, operating in the near-infrared range, have been proposed to quantify scatter in cataract patients<sup>26</sup> and in dry eye cases.<sup>27</sup> Although, as shown here, the impact of diffusion at the fundus could be very significant, it should be noted that those studies were dealing with relative comparisons of a highly elevated

amount of scatter, produced either by the cataractous lenses or by the malfunctioning tear film. Therefore, although near infrared can be used to assess scatter in low-transparency eyes, shorter wavelengths should be used to assess scatter in normal eyes.

In conclusion, the central part of the wide-angle PSF in the eye is affected by the wavelength-dependent properties of the diffuse reflectance of the fundus, which are also related to the

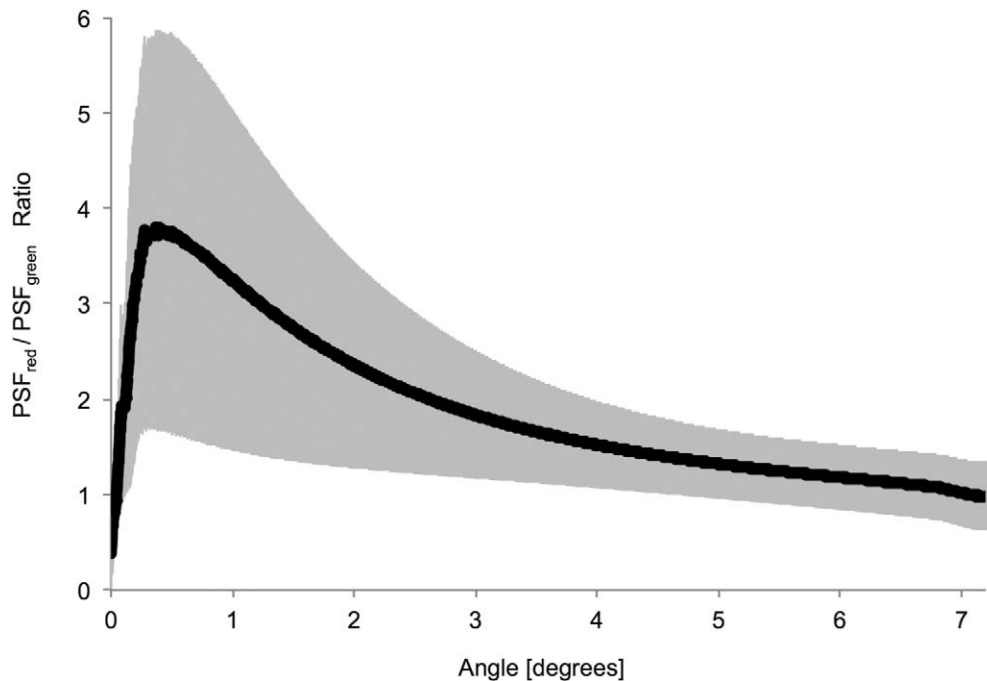


FIGURE 8. Ratio of the PSF at “red” wavelengths to the PSF at “green” wavelengths. *Gray area* corresponds to 2 standard deviations (across subjects).

subject's pigmentation. At those small angles, measurements using wavelengths shorter than 600 nm might be better correlated with straylight affecting vision. However, the impact of diffusion at the fundus on the values of the straylight parameter at larger angles did not depend on the measuring wavelength. There, absolute minimum of straylight occurs at approximately 550 nm, possibly as a combined effect of increased scattering in the optics of short wavelengths and increased diffusion at the fundus of longer wavelengths.

### Acknowledgments

Supported by Ministerio de Educación y Ciencia, Spain (Grants FIS2010-14926 and Consolider Program SAUUL CSD2007-00013); EU ITN OpAL (PITN-GA-2010-264605); and Fundación Séneca, Murcia, Spain (Grant 04524/GERM/06).

Disclosure: **H.S. Ginis**, P; **G.M. Perez**, P; **J.M. Bueno**, P; **A. Pennos**, None; **P. Artal**, P

### References

- Holladay LL. The fundamentals of glare and visibility. *J Opt Soc Am*. 1926;12:271-319.
- Vos JJ. Disability glare—a state of the art report. *CIE J*. 1984;3/2:39-53.
- Ijspeert JK, de Waard PWT, van den Berg TJTP, de Jong PTVM. The intraocular straylight function in 129 healthy volunteers: dependence on angle, age and pigmentation. *Vision Res*. 1990;30:699-707.
- van den Berg TJ, Ijspeert JK, de Waard PW. Dependence of intraocular straylight on pigmentation and light transmission through the ocular wall. *Vision Res*. 1991;31:1361-1367.
- van de Kraats J, Berendschot TT, van Norren D. The pathways of light measured in fundus reflectometry. *Vision Res*. 1996;36:2229-2247.
- van den Berg T, Tan K. Light transmittance of the human cornea from 320 to 700 nm for different ages. *Vision Res*. 1994;34:1453-1456.
- Thaung J, Sjöstrand J. Integrated light scattering as a function of wavelength in donor lenses. *J Opt Soc Am A Image Sci Vis*. 2002;19:152-157.
- van den Berg TJ, Ijspeert JK. Light scattering in donor lenses. *Vision Res*. 1995;35:169-177.
- Wooten B, Geri G. Psychophysical determination of intraocular light scatter as a function of wavelength. *Vision Res*. 1987;27:1291-1298.
- Whitaker D, Steen R, Elliott DB. Light scatter in the normal young, elderly, and cataractous eye demonstrates little wavelength dependency. *Optom Vis Sci*. 1993;70:963-968.
- Franssen L, Coppens JE, van den Berg TJTP. Compensation comparison method for assessment of retinal straylight. *Invest Ophthalmol Vis Sci*. 2006;47:768-776.
- Coppens JE, Franssen L, van den Berg TJTP. Wavelength dependence of intraocular straylight. *Exp Eye Res*. 2006;82:688-692.
- Ijspeert JK, van den Berg TJTP, Spekrijse H. An improved mathematical description of the foveal visual point spread function with parameters for age, pupil size and pigmentation. *Vision Res*. 1993;33:15-20.
- Vos JJ, van den Berg TJTP. Report on disability glare. *CIE Collection*. 1999;135:1-9. Available at: <http://www.nin.knaw.nl/Portals/0/Department/Berg/Documents/VosAvdB1999.pdf>.
- Stiles WS. The effect of glare on the brightness difference threshold. *Proc Roy Soc*. 1929;104B:322-355.
- van den Berg TJTP. Analysis of intraocular straylight, especially in relation to age. *Optom Vis Sci*. 1995;72:52-59.
- Ginis H, Perez GM, Bueno JM, Artal P. The wide-angle point spread function of the human eye reconstructed by a new optical method. *J Vis*. 2012;12:20.
- Santamaria J, Artal P, Bescos J. Determination of the point-spread function of human eyes using a hybrid optical-digital method. *J Opt Soc Am A*. 1987;4:1109-1114.
- Vos JJ, Walraven J, van Meeteren A. Light profiles of the foveal image of a point source. *Vision Res*. 1966;16:215-219.
- Walraven J. Spatial characteristics of chromatic induction: the segregation of lateral effects from straylight artefacts. *Vision Res*. 1973;13:1739-1753.
- Berendschot T, DeLint P, van Norren D. Fundus reflectance—historical and present ideas. *Prog Retin Eye Res*. 2003;22:171-200.
- Delori F, Pflibsen K. Spectral reflectance of the human ocular fundus. *Appl Optics*. 1989;28:1061-1077.
- Hodgkinson IJ, Greer PB, Molteno AC. Point-spread function for light scattered in the human ocular fundus. *J Opt Soc Am A Opt Image Sci Vis*. 1994;11:479-486.
- Kienle A, Patterson MS. Improved solutions of the steady-state and the time-resolved diffusion equations for reflectance from a semi-infinite turbid medium. *J Opt Soc Am A Opt Image Sci Vis*. 1997;14:246-254.
- Berendschot TJ, van de Kraats J, van Norren D. Wavelength dependence of the Stiles-Crawford effect explained by perception of backscattered light from the choroid. *J Opt Soc Am A Opt Image Sci Vis*. 2001;18:1445-1451.
- Artal P, Benito A, Pérez GM, et al. An objective scatter index based on double-pass retinal images of a point source to classify cataracts. *PLoS One*. 2011;6:e16823.
- Benito A, Perez GM, Mirabet S, et al. Objective optical assessment of tear-film quality dynamics in normal and mildly symptomatic dry eyes. *J Cataract Refract Surg*. 2011;37:1481-1487.